MAGNETORHEOLOGICAL FLUID BRAKE – BASIC PERFORMANCES TESTING WITH MAGNETIC FIELD EFFICIENCY IMPROVEMENT PROPOSAL

A. Poznić[1⊠], A. Zelić[1], L. Szabó[2]

[1]University of Novi Sad, 6 Trg Dositeja Obradovića, 21 000 Novi Sad, SERBIA
⊠E-mail: alpoznic@uns.ac.rs
[2]University of Pannonia, 18 Zrínyi Str., 8800 Nagykanizsa, HUNGARY

A review of all magnetorheological brake types was presented. Based on overall braking torque analytical comparison for all magnetorheological brake types and other relevant parameters, the most promising design was selected. A test rig, utilizing selected brake type filled with magnetorheological fluid – Basonetic 5030 was manufactured and then tested. To analyze the effect produced by magnetic field on magnetorheological fluid and hence at overall braking torque, the authors used amplification factor. Results were discussed and the magnetic field efficiency improvements were proposed.

Keywords: magnetorheological brake, Basonetic 5030, test rig, amplification factor, efficiency improvements

Introduction

The convectional friction brake (FB) is the most commonly used brake type in almost any mechanical system today. However, it is characterized by drawbacks such as periodic replacement due to wear, large mechanical time-delay, bulky size etc. [13, 29], partially altered. Electromechanical brakes (EMBs) have potential to overcome some of these drawbacks and are a suitable FB replacement. Today EMBs are applicable in almost any mechanical system. Application of intelligent materials is the next step in the development of EMB.

Magnetorheological (MR) fluids belong to a class of intelligent materials that respond to applied magnetic field with fast, continuous, and reversible change in its rheological behaviour [3, 7, 28], partially altered. MR fluids are a type of suspensions, with carrier fluid usually mineral or synthetic oil, water, kerosene and micro size magnetizable particles dispersed in it. When exposed to external magnetic field particles form a chain-like structures thus changing the viscosity of the fluid. In this study, authors used BASF's magnetorheological fluid, Basonetic 5030.

MR fluids have attracted extensive research interest in recent years since they can provide simple, quiet and fast response interface between electronic control and mechanical system [11, 20, 22]. A lot of work was done on MR fluid brakes modelling, properties investigation and control [3, 6, 11]. A wide range of MR fluid devices have also been investigated for their potential applications in different systems, such as: clutch system, vibration control, seismic response reduction, etc. [9, 10, 26].

MR fluid brakes have also been used in actuators due to their distinguished force control and power transmission features [5, 15]. By applying a proper control effort, viscosity with large varying range is achievable with the MR fluid brake. Currently, there are many solutions for MR fluid brake design. Some MR fluid brakes with attractive properties, such as high yield stress and stable behavior, have been developed and commercialized [4, 16].

The objective of this work was to compare overall braking torque analytical expressions and design complexity for all MR fluid brake types. Based on results obtained from these comparisons, MR fluid brake type with the most promising properties was manufactured and tested on a specially designed test rig. Results were discussed and a proposal for new MR brake design with higher magnetic efficiency was presented.

Magnetorheological effect

MR fluids are suspensions composed out of three major components: carrier fluid - usually mineral or synthetic oil, magnetizable particles - carbonyl iron powder and set of additives [2, 17], partially altered. When exposed to an external magnetic field (ON state), change in MR fluid's viscosity occurs. In the absence of an external magnetic field (OFF state), MR fluid acts as Newtonian fluid [7, 11] and can be described as:

$$\tau = \eta \cdot \dot{\gamma} \tag{1}$$

In (1) τ represents shear stress, η the viscosity of the fluid and $\dot{\gamma}$ shear rate. Often, for MR fluid brakes,

114

denoted as $\dot{\gamma} = r \cdot \omega / g$, where r is rotor radius, ω and g are angular speed and MR fluid gap length, respectively.

When in ON state, MR the rheological properties of MR fluid change. Magnetizable particles induce polarization and form chain-like structures in magnetic flux path direction, thus changing apparent viscosity of the fluid. ON state behavior of MR fluid is often represented as a non-Newtonian [1, 3, 5], having a variable yield strength. The usage of Bingham's model (2), in this situation, gives reasonably good results, [1, 11, 20, 22]:

$$\tau = \tau_B + \eta \cdot \dot{\gamma}, \qquad (2)$$

where τ_B is the yield stress, developed in response to the applied magnetic field. Its value is a function of the magnetic field induction B.

When used in a device, MR fluid can be in one of four modes: shear, flow (pressure), squeeze and pinch, [8, 18, 28]. In brake i.e. torque transfer applications, MR fluid operates in shear mode [1]. Braking torque values are adjusted continuously by changing the external magnetic field strength.

Magnetorheological brakes

MR brake consists out of four main parts: rotor, housing i.e. stator, coil and MR fluid, *Figure 1*. The shape of the rotor is what differentiates MR brake types from each other. One needs the quantitative parameters of MR brake, to be able to determine its specific application suitability.

MR brake types, mechanical model, quantitative parameters comparison for all MR brake types are presented in next section.

Magnetorheological brake types

Through literature research [9, 14, 22, 23, 24], authors of this paper have identified five major MR fluid brake designs: drum brake, inverted drum brake, disk brake, T-shape rotor brake and multiple disks brake, *Fig. 1*.

Drum brake along with the disk brake is the easiest designs to manufacture. However, large inertia is its major drawback compared to disk brake design [1].

The disk brake design is the most common MR brake design found in literature today and was the first one to be investigated [25]. It is the easiest one to manufacture and gives reasonably good results in terms of weight and compactness [14]. There are some variations in MR disk brake design such as: the use of two coils instead of one in order to increase the magnetic pole area and/or relocation of the coil on top of the disk in order to reduce its external diameter [22], but the basics remain the same. It is also interesting to note that the MR disk brake design is currently the only one commercially available as a standard product, manufactured by Lord Corporation [16] and that it was used in several studies [7, 19, 21].

In order to increase compactness of the MR disk brake design, several disk-shape rotors can be used instead of one, with segments of stator located in between each rotor disk, *Fig. 1.d*. This multiple disk design is very popular in literature and was used in several applications that required high torque in limited space and weight [13, 22, 23]. The equations describing this particular design are very similar to those of the single disk brake, presented paper's sequel.

The T-shape rotor brake design *(Fig. 1.e)*, is more compact than all other designs but is also more complex to manufacture. Despite its advantages, this design is not so common in literature [22].
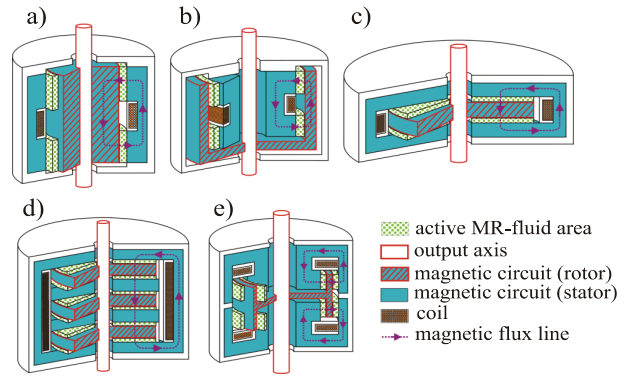

Figure 1: Types of MR brakes: a) drum, b) inverted drum, c) disk, d) multiple disks, e) T-shaped rotor, [28]

For all aforementioned MR brake types, the rotor has a cylindrical shape and the magnetic flux lines run in the radial direction, *Fig. 1*.

To author's knowledge, an in-depth comparison of all these architectures is not yet available.

Mechanical model

The key objective in MR fluid brake design is to establish the relationship between the overall braking torque, magnetic field strength and design parameters. Interaction of MR fluid and inner surfaces of the brake will generate the braking torque. Based on *Eq. (2)* and the specific geometrical configuration of MR brake, for all MR brake types, it applies:

$$dT = 2\pi N \tau r^2 dr, \qquad (3)$$

where:

N – number of surfaces of the rotor, perpendicular to the magnetic flux lines and in contact with MR fluid,

r – the radius of the rotor.

The overall braking torque $T_{Overall}$, consists of three components:
- the magnetic field induced component T_B, due to the field-dependent yield stress,
- the fluid viscosity dependent component T_{vis} and
- the friction induced component $T_{fric.}$.

Thus, the overall brake torque:

$$T_{Overall} = T_B + T_{vis} + T_{fric} \qquad (4)$$

The sum of the first two components T_B and T_{vis} i.e. the braking torque can be obtained by the following integral:

$$T_B + T_{vis} = 2\pi N \int_{R_i}^{R_o} \tau r^2 \mathrm{d}r , \qquad (5)$$

where R_O and R_i are the brake's rotor outer and inner radii respectively. Considering practical conditions, for all MR brake types, the value of the R_i can be ignored because the R_O is several order of magnitude of the R_i (Figure 2).
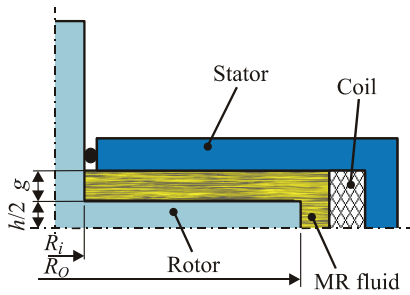

Figure 2: MR fluid disk brake simplified representation

Based on *Eq. (5)*, the authors formed the final analytical expressions for all five MR brake designs. Expressions were adopted from several different literature sources [1, 6, 12, 13, 21, 27, 29] and were partially altered in order to make the comparison easier. The last part of torque, T_{fric} can be precisely obtained only by torque gauge.

$$T_{Overall} = \pi(\frac{4}{3}\tau R_O^3 + \eta\frac{\omega}{g}R_O^4) + T_{fric} , \qquad (6)$$

$$T_{Overall} = \pi N(\frac{4}{3}\tau R_O^3 + \eta\frac{\omega}{g}R_O^4) + T_{fric} , \qquad (7)$$

$$T_{Overall} = 4\pi h(\tau R_O^2 + \eta\frac{\omega}{g}R_O^3) + T_{fric} , \qquad (8)$$

$$T_{Overall} = 8\pi h(\tau R_O^2 + \eta\frac{\omega}{g}R_O^3) + T_{fric} . \qquad (9)$$

Variable h is the height of the rotor.

It is now easy to distinguish components of overall braking torque in *Eq. (6–9)*, for disk, multiple disks, drums and T-shaped rotor, respectively. The yield stress τ_B given in *Eq. (2)*, varies with magnetic induction, but can reasonably be fitted with the third-order polynomial [12], as follows:

$$\tau_B = K_1 B + K_2 B^2 + K_3 B^3 , \qquad (10)$$

where K_i represents coefficients of regression.

Performances comparison

MR brakes can be compared on several different aspects e.g. overall braking torque, dynamic range, mechanical simplicity, inertia, electric power consumption, torque to volume ratio, compactness, etc. Authors of this paper compared level of mechanical simplicity for all five MR brake types and the overall braking torque based on analytical expressions, given in *Eq. (6–9)*, *Table 1*. In addition, the dynamic range and inertia were consider and presented in the same table.

Table 1: Characteristics of various MR brake designs

Brake type	$T_{Overall}$	Level of mechanical simplicity	Dynamic range T_B/T_{vis}	Inertia
(1)	M	H	$\dfrac{\tau_B}{\eta\dot\gamma}\cdot\dfrac{g}{R_i}$	$\dfrac{1}{2}mR_O^2$ *
(2)	M	L	$\dfrac{4}{3}\cdot\dfrac{\tau_B}{\eta\dot\gamma}\cdot\dfrac{g}{R_O}$	$\dfrac{1}{2}mR_O^2$
(3)	H	L	$\dfrac{4}{3}\cdot\dfrac{\tau_B}{\eta\dot\gamma}\cdot\dfrac{g}{R_O}$	$\dfrac{1}{2}mR_O^2 N_D$
(4)	H	H	$\dfrac{\tau_B}{\eta\dot\gamma}\cdot\dfrac{g}{R_O}$	$mR_O^2 - \dfrac{m_i R_i^2}{2}$

Explanations:
Brake types: (1) drum and inverted drum, (2) disk, (3) multiple disks, (4) T-shaped rotor.
Level of mech. simplicity: H – high, M - medium, L – low.
* For inverted drum brake design, expression is the same as for the T-shape rotor design.
N_D – the number of rotor disks, m_i – missing inner mass of the disk.

Dynamic range represents ratio of field induced component T_B and viscous component T_{vis} (friction torque component not considered).

T-shaped rotor brake performs best dynamic and can offer biggest overall braking torque, however it has a large inertia, and is considered difficult to manufacture. The other four designs are globally less compact than the T-shaped rotor design. The two drum based designs have comparable performances but are burdened with even larger inertia for same rotor radius. Finally, the disk and multiple disks designs offer a good alternative, being mechanically the simplest, with smaller inertia and giving reasonable dynamic range and the overall braking torque.

Test rig

Based on test rigs literature research [10, 15, 20, 27] and MR brake properties comparison *(Eq. (6–9)* and *Tab. 1)*,

the authors of this paper selected the most promising MR brake design and manufactured it. With lowest inertia, good dynamic range and the highest mechanical simplicity, the disk type promised the biggest potential.

For performance evaluating of the selected MR brake type a rig was set up. The test rig was designed and manufactured at Faculty of technical sciences, Novi Sad – Serbia, and is presently at its Laboratory for engines and vehicles. The test rig with its parts is depict in *Figure 3 and 4*, and consists of four main parts:

- drive,
- power supply,
- MR brake and
- measuring and data acquisition equipment.

An 8-pole AC squirrel cage motor with 0.75 kW and nominal speed of 700 rpm, model 5 AZ 100 LA – 8 (*Končar*) was placed at one end of the support-frame, of the test rig. The inverter - Micro Master (*Siemens*), *Fig. 4*, position 2, controls the direction and variable-speed of the AC motor. Speed range was from 150 rpm to 750 rpm with 50 rpm increment. These two elements form a drive part of the test rig. The flexible coupling connects AC motor and the shaft of the MR brake. MR brake rests on two self-aligning ball bearings into housings P203 (*FK Bearing group*). To avoid leakage of MR fluid, Nitrile Rubber lip seals, suitable for MR type application, have been used.

Torque transfer from the MR brake to a measurement device was done indirectly. A load arm, connected to the MR brake housing at one end, rests on top of the load cell on the other end, *Fig. 3*. Thus, by measuring the force on the load cell, the value of transmitted torque was obtained. Load cell was internally calibrated by calibration weights. The capacity of the load cell, 1030 (*Tedea*), was 15 kg.
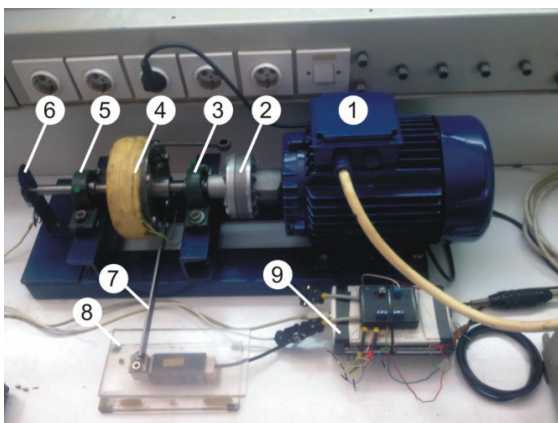

Figure 3: Demonstrating the test rig for MR brake
1. drive, 2. coupling, 3. self-aligning ball bearing, 4. MR fluid brake, 5. self-aligning ball bearing, 6. optical encoder, 7. load arm, 8. load cell, 9. data acquisition card

The optical encoder, model AMT102-V-REV-C (*CUI Inc.*), was connected to the shaft of the MR brake, at the opposite side of the AC motor and rotated at the same speed sample rate was 2048 per rotation. The signals were processed by universal amplifier, KWS

673.A2 (*HBM*), *Fig. 4*, position 3. The DC power supply, EA PS 2016-100 (*Elektro-automatik*), was connected to the leads of the coil to provide flux generation. This was the control current, with range of 0 A to 2 A and 0.2 A increment. The coil, made of copper wire with diameter of 1 mm (18 gauges) has been coiled on outer radius of the MR brake housing.

The MR fluid used in this experiment was Basonetic® 5030, from BASF® [17]. It is a carbonyl iron powder based MR fluid.

Figure 4: Measurement and data acquisition equipment: 1. stabilized power supply, 2. inverter, 3. universal amplifier

A typical testing procedure was as follows. First, the MR brakes shaft was set to a certain speed for 1 min as an initial condition, which stirred the MR fluid in the brake to distribute it uniformly. The desired magnetic field was then applied by setting the coil current i.e. control current and waiting for 1 min. This ensured stable structure forming of the MR fluid. The load cell detected transmitted torque. Finally, the signal from the load cell was processed and recorded.

Experimental results and improvement proposal

The goal of this experiment was to determine overall braking torque capabilities of selected MR brake design. The experiment was conducted on a specially designed test rig, with different control currents and speed sets. To eliminate the effects of previous observations, different combinations of control current and rotational speed were set for each reading. To bring repeatability in the reading, every speed set was carried out twice at different instance of time. For every reading, approximately 1 min time, before torque data recording, has been allotted to distribute the carbonyl iron particles uniformly in the MR fluid and form a stable structure.

Experimental results

The experiment itself consisted out of tree parts. The first part was to determine the influence of the supporting ball bearings and seals, without MR fluid inside the brake and no control current applied. This was a friction braking torque component. Second part of the experiment had the same setup but it included MR fluid inside the brake. Viscous torque data was then

recorded, assuming that bearings and seals did not change their friction characteristics in time.

Aforementioned recordings were needed in order to get clear and precise information about field induced component. This was the third part of the experiment and it included MR fluid inside the brake and application of the control current.

The same speed sets were used for the friction and the viscous torque component measurements were repeated. For each speed set, a 2 minute recording time was used. Some field induced component results are depict in *Figure 5*. Magnetic field influence is apparent.
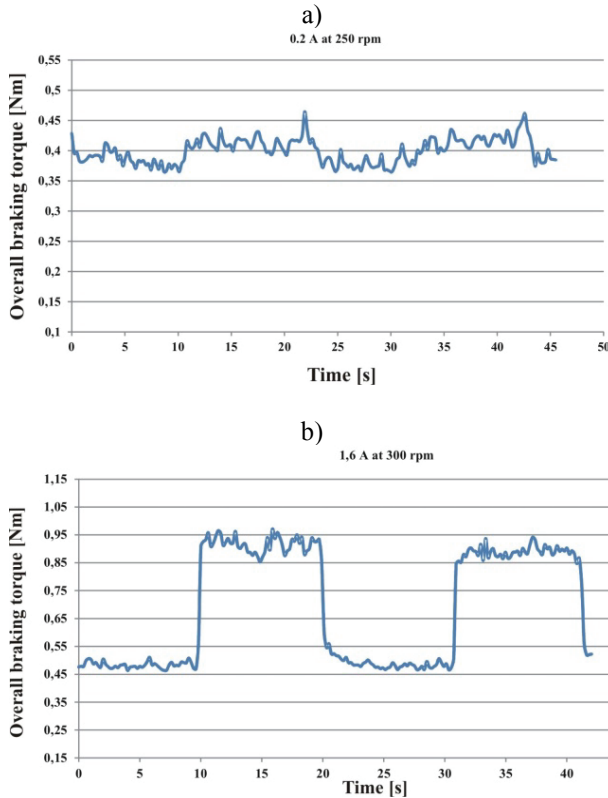

a)

b)

Figure 5: Samples of overall braking torque results: a) 0,2 A at 150 rpm, b) 1,6 A at 300 rpm

Because of the large number of data obtained in this experiment, authors decided to use amplification factor to determine the effect produced by magnetic field. Amplification factor (AF) represents relation between overall braking torque and sum of friction and viscous torque, i.e. relation between the ON and OFF state of the MR fluid.

$$AF = \frac{T_{Overall} \text{ at current } I}{T_{Overall} \text{ at zero current}} \qquad (11)$$

Amplification factor curves for all 13 speed sets are plotted in *Figure 6*. This figure shows linearity in amplification factor with increase in control current. This was expected, since the higher the current, the higher the field induced torque should be. Results are presented with rotational speed variation as well.

Figure 6 indicates that the amplification factors for speeds 150, 200, 250, 300 and 350 were much larger than the ones for 450, 500, 550, 600, 650, 700 and 750 rpm.

Transition rpm value for this MR brake was 400 rpm. This was somewhat opposite to the torque predicted by *Eq. (6)* where the $T_{Overall}$ should increase with angular speed. This was not the case here. However, other authors have also reported the same trend – reduction of amplification factor with increment of speed [20, 27]. This may be due to the possible shear thinning effect of the MR fluid at high shear rates. This reduces the effectiveness of MR brake at higher speeds. Therefore, to make MR brake effective at higher speed operation, one needs to think of „Shear stable MR fluid".
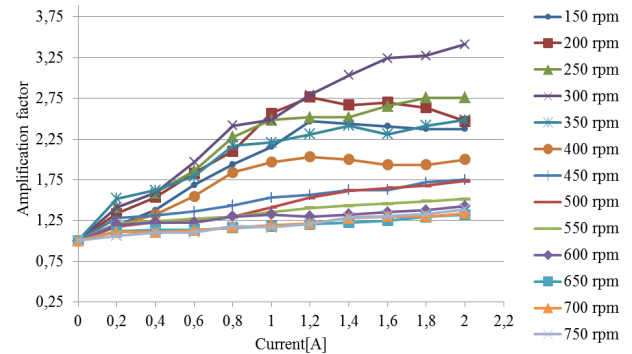

Figure 6: Variation in amplification factor with control current

MR brake improvement proposal

In order to increase the overall braking torque of any MR brake type its geometry needs to be optimized [14]. State of the art MR brake designs base their torque generation on the inner section of the coil [4, 10, 13]. These designs are rather inefficient, because the magnetic field is not used to its full potential and active MR area is small. Flux mostly travels through the housing of the MR brake. In this configuration, magnetic field is concentrated on small area of the MR fluid.
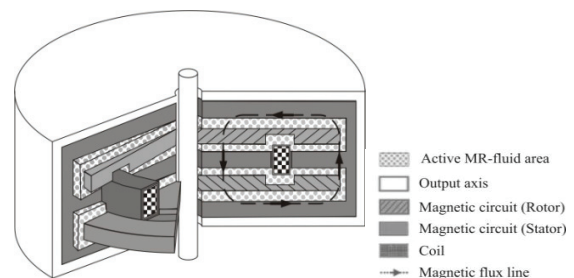

Figure 7: Novel MR brake design with enhanced magnetic field efficiency

By altering earlier MR brake designs, it is possible to concentrate magnetic field effect. One such design has been presented in *Figure 7*.

Compared to the dimensions of the tested MR disk brake, radius of the coil was reduced so that it could be placed in a more suitable position inside new MR brake design. New coil position allows for magnetic flux to be

118

used more efficiently. Now, the magnetic flux inside MR brake passes through MR fluid several times.

Based on analytical comparison, presented in *Eq. (6–9)* and *Tab. 1*, new design features two disks in order to create more MR fluid active area. Greater number of disks creates more MR fluid gaps thus the volume of MR fluid can be increased.

Conclusion

Authors compared all MR brake types on several different aspects. Based on this information, the most promising MR brake type was selected, manufactured and tested on a specially designed test rig.

The MR brake produced desirable results, which coincide with literature sources. Approximately linear relation between the overall braking torque and the control current intensity was observed. To present results in more readable manner, the amplification factor was introduced.

The experiment showed that the tested MR brake has potential for practical applications due to easiness and accuracy of control. However, the value of the overall braking torque is still small. To increase it, better utilization of the existing magnetic field is needed. The authors suggested different approach in comparison to the conventional MR brake design that would increase the overall braking torque by increasing the magnetic field efficiency and the contact area of the MR brake fluid. By multiplying the number of the disks in contact with MR fluid, value of the overall braking torque will multiply as well, *Eq. (7)*.

In order to maximize the potential of the proposed MR brake, further investigations on magnetic field propagation is needed as well as design optimization. Finite element method model of the novel MR brake is the next step in this process.

Acknowledgments

REFERENCES

1. T. M. AVRAAM: MR-fluid brake design and its application to a portable muscular rehabilitation device, PhD thesis, Active Structures Laboratory, Department of Mechanical Engineering and Robotics, Universit´e Libre de Bruxelles, Bruxelles (2009)

2. G. BOSSIS, S. LACIS, A. MEUNIER, O. VOLKOVA: Magnetorheological fluids, Journal of magnetism and magnetic materials, 252 (2002), pp. 224–228

3. J. D. CARLSON, M. R. JOLLY: MR fluid, foam and elastomer devices, Mechatronics, 10 (2000), pp. 555–569

4. J. D. CARLSON, D. M. CATANZARITE, K. A. CLAIR: Commercial magnetorheological fluid devices, In Proceedings of the 5th International Conference on ER Fluids, MR Suspensions and Associated Technology (Ed. W. A. Bullogh), Singapore (1996), pp. 20–28

5. E. D. ERICKSEN, F. GORDANINEJAD: A magneto-rheological fluid shock absorber for an off-road motorcycle, International J. Vehicle Design, 33 No 1-3 (2003), pp. 139–152

6. A. FARJOUD, N. VAHDATI, Y. F. FAH: Mathematical model of drum-type MR brake using Hershel-Bulkley shear model, Journal of Intelligent Material Systems and Structures (2007), pp. 1–8

7. D. G. FERNANDO: Characterizing the behavior of magnetorheological fluids at high velocities and high shear rates, PhD thesis, Faculty of the Virginia Polytechnic Institute and state University, Blacksburg,Virginia (2005)

8. F. D. GONCALVES, J. D. CARLSON: An alternate operation mode for MR fluids – Magnetic Gradient Pinch, Journal of Physics: Conference Series, 149 (2009), pp. 1–4

9. K. H. GUDNUNDSSON, F. JONSDOTTIR, F. THORSTEINSSON: A geometrical optimization of a magneto-rheological rotary brake in a prosthetic knee, Smart Materials and Structures, 19 (2010) pp. 1–11

10. Z. HEROLD, D. LIBL, J. DEUR: Design and testing of an experimental magnetorheological fluid clutch, Strojarstvo, 52 No. 3 (2010), pp. 601–614

11. J. HUANG, J. Q. YHANG, Y. YANG, Y. Q. WEI: Analysis and design of a cylindrical magneto-rheological fluid brake, Journal of Material Processing Technology, 129 (2002) pp. 559–562

12. A. JINUNG, K. DONG-SOO: Modelling of mag-netorheological actuator including magnetic hysteresis, Journal of Intelligent Material Systems and Structures, 14 (2003) pp. 541–550

13. K. KARAKOC, J. E. PARK, A. SULEMAN: Design considerations for an automotive magnetorheo-logical brake, Mechatronics, 18, No. 8 (2008), pp. 434–447

14. K. KARAKOC: Design of a Magnetorheological Brake System Based on Magnetic Circuit Optimization, PhD Thesis, Department of Mechanical Engineering, University of Victoria, Victoria, Canada (2007)

15. B. M. KAVLICOGLU, F. GORDANINEJAD, C. A. EVRENSEL, N. COBANOGLU, Y. LUI, A. FUCHS, G. KOROL: A high-torque magneto-rheological fluid clutch, Proceedings of SPIE Conference on smart

materials and structures, March 2002, San Diego, pp. 1–8

16. K. KAYLER: Lord corporation expands production of steer-by-wire TFD brakes to meet demand, available from: http://www.lord.com/news-center/press-releases/lord-corporation-expands-production-of-steer-by-wire-tfd-brakes-to-meet-demand-.xml. (Accessed on 6. 20. 2013.)

17. C. KIEBURG: MR-fluid Basonetic 5030, Technical Information, BASF SE Metall Systems, Ludwingshafen, Germany (2010)

18. U. LANGE, L. RICHTER, L. ZIPSER: Flow of magnetorheological fluids, Journal of Intelligent Material Systems and Structures, 12 (2001), pp. 161–164

19. D. LAMPE, R. GRUNDMANN: Transitional and solid state behaviour of a magnetorheological clutch. In Proceedings of Actuator 2000, Bremen (2000)

20. W. H. LI, H. DU: Design and experimental evaluation of a magnetorheological brake, The International Journal of Advanced Manufacturing Technology, 21 (2003), pp. 508–515

21. B. LIU, W. H. LI, P.B. KOSASIH, X. Z. ZHANG: Development of an MR-brake-based haptic device, Smart Materials and Structures, 15 (2003), pp. 1960–1966

22. Q. N. NGUYEN, S. B. CHOI: Selection of magnetorheological brake types via optimal design considering maximum torque and constrained volume, Smart Materials and Structures, 21 (2012), pp. 1–12

23. E. J. PARK, D. STOIKOV, L. F. DA LUZ, A. SULEMAN: A performance evaluation of an automotive magnetorheological brake design with a sliding mode controller, Mechatronics, 16 (2006), pp. 405–416

24. N. PHUONG-BAC, C. SEUNG-BOK: A new approach to magnetic circuit analysis and its application to the optimal design of a bi-directional magnetorheological brake, Smart Materials and Structures, 20 (2011), pp. 1–12

25. J. RABINOW: Magnetic fluid torque and force transmitting device, US patent 2,575,360, 1951.

26. B. F. SPENCER, S. J. DYKE, M. K. SAIN, J. D. CARLSON: Phenomenological model of a magnetorheological damper, ASCE Journal of Engineering Mechanics, 123, No. 3 (1996), pp. 1–23

27. V. K. SUKHWANI, H. HIRANI: Design, development, and performance evaluation of high-speed magnetorheological brakes, Proceedings of the Institution of Mechanical Engineers, Part L: Journal of Materials Design and Applications, 222 (2008), pp. 73–82

28. J. WANG, G. MENG: Magnetorheological fluid devices: principles, characteristics and applications in mechanical engineering, Proceedings of Institution of Mechanical Engineers – Part L – Journal of Materials: Design and Application, 215 (2001), pp. 165-174

29. Z. A. ZAINORDIN, A. M. ABDULLAH, K. HUDHA: Experimental evaluations on braking responses of magnetorheological brake, International journal of mining, metallurgy & mechanical engineering, 1, No. 3 (2013), pp. 195–199